Journal of Intelligent & Robotic Systems (2024) 110:13
https://doi.org/10.1007/s10846-023-02031-w

REGULAR PAPER

Multimodal Interaction Strategies for Walker-Assisted Gait: A Case Study for Rehabilitation in Post-Stroke Patients

Mario F. Jimenez[1] · Ricardo C. Mello[2] · Flavia Loterio[2] · Anselmo Frizera-Neto[2]

Received: 21 February 2023 / Accepted: 7 December 2023 / Published online: 16 January 2024

Abstract

Stroke has been considered the main cause of neuromuscular damages worldwide and one of the most common causes of walking disabilities, with approximately 60% of the individuals suffering from persistent problems in walking. These patients generally use technical aids for walking to achieve independent gait, however, when cognitive impairments are also present, conventional assistive devices such as walkers could be difficult to handle. By leveraging multimodal interfaces, smart walkers can offer natural and intuitive human-robot interaction. In this work, we present two multimodal interaction strategies for smart walkers focusing on guiding post-stroke patients through their environment. These strategies leverage different communication channels and provide distinct levels of guidance: one strategy uses haptic feedback and a visual interface to indicate the desired path to the user, while the other strategy uses haptic feedback and a virtual torque to maintain the user on path. We also present two case studies with post-stroke patients to preliminarily validate these interaction strategies with their target population and to collect valuable insight as to how multimodal strategies for smart walkers can be enhanced to deal with the characteristic asymmetries of post-stroke patients. Our results show that both strategies can guide the volunteers, however, the first one demands more effort from the volunteer and is more suited for patients with increased levels of independence. The second interaction strategy allows for higher linear velocity (Volunteer 1, $\mathbf{0.18 \pm 0.026}$ $\boldsymbol{m/s}$; Volunteer 2, $\mathbf{0.22 \pm 0.0283}$ $\boldsymbol{m/s}$) than the first one (Volunteer 1, $\mathbf{0.10 \pm 0.031}$ $\boldsymbol{m/s}$; Volunteer 2, $\mathbf{0.20 \pm 0.012}$ $\boldsymbol{m/s}$), suggesting improved guidance.

Keywords Post-stroke · Assistance robotics · Admittance control · Haptic feedback · Smart walker

1 Introduction

Stroke has been considered the main cause of neuromuscular damages worldwide, and one of the most common causes of walking disabilities, with approximately 60% of the individuals suffering from persistent problems in walking [1, 2]. As a consequence of stroke, the individual also presents significant asymmetry in joint kinematics, abnormal muscle activation, and impaired postural control [2, 3].

Ricardo C. Mello, Flavia Loterio and Anselmo Frizera contributed equally to this work

✉ Mario F. Jimenez
mariof.jimenez@urosario.edu.co

Ricardo C. Mello
ricardo.c.mello@ufes.br

Flavia Loterio
loteriofa.ufes@gmail.com

Anselmo Frizera-Neto
frizera@ieee.org

1 School of Engineering, Science and Technology, Universidad del Rosario, Bogotá 111711, Colombia

2 Graduate Program in Electrical Engineering, Federal University of Espírito Santo, Vitoria 29075-910, Brazil

Most post-stroke subjects need rehabilitation, mainly aiming to independence improvement, for instance gait recovery [4]. An incomplete recovery not only maintains the abnormal pattern of the paretic limb, but can also impair the contralateral limb, due to the constant presence of compensatory mechanisms during gait, and cause secondary complications because of mobility decreased [5, 6]. These patients generally use technical aids for walking, as they improve symmetry, stability and balance [7, 8].

Conventional walkers, in particular, can be used to assist post-stroke patients during rehabilitation. Such devices are available in several configurations (i.e., 4-tips, 2-wheel, and 4-wheel), which are prescribed according to the needs of the user [9]. Despite empowering human locomotion, conventional walkers do not eliminate the risk of falling and might not be able to assure safety for severely impaired users [9, 10]. Moreover, when cognitive impairments are also present, the handling of conventional walkers can become a complex task. Conventional walkers are also incapable of providing cognitive assistance and lack features such as navigation assistance. These issues can be mitigated by the integration of robotics with conventional walkers. Such robotic devices, also known as smart walkers (SW), are able to provide physical support, sensorial assistance, cognitive assistance, and health monitoring [10, 11].

SW can leverage the use of multimodal interfaces to interact with the user and to detect human motion intentions with high precision [12–14]. Moreover, when the user presents gait asymmetry, the use of multiple interfaces gathers a more inclusive set of data that can be used by the SW controllers. This leads to a natural and intuitive human-robot interaction (HRI), which can improve user experience [15, 16]. Moreover, by perceiving its surroundings, the SW may leverage contextual information to improve the conventional HRI towards a human-robot-environment interaction (HREI) [11].

The literature describes several multimodal interaction strategies for smart walkers, but fewer studies have been conducted with focus on validating these strategies with mobility impaired individuals. Studies relating the use of smart walker in therapy are usually focused on biomechanical parameters and do not discuss interaction aspects (e.g., [17, 18]). In Jimenez et al. [13] and in Jimenez et al. [14] our group presented and validated multimodal interaction strategies focusing on validating the interaction and its functionality. In this work, we validate the interaction strategies presented in [13] and [14] with post-stroke individuals.

The main contribution of this work is the conduction of two case studies with mobility impaired individuals and the subsequent evaluation of two multimodal interaction strategies. We present two case studies with post-stroke patients using a smart walker considering two different multimodal interaction strategies. One interaction strategy, functionally validated in Jimenez et al. [13], is based on three interaction channels: haptic feedback, resulting from the physical contact between user and SW; a visual interface, which hints paths to follow as chosen by the therapist; and a supervisor that monitors user parameters to enforce pre-established safety rules. As for the other strategy, which was functionally validated in Jimenez et al. [14], the path to follow is indicated by the haptic feedback, thus removing the visual interface. The post-stroke patients present different levels of impairments, which reflected in the way they could interact with the SW. We discuss our findings and suggest future research directions in the field of SW for development of modern neurorehabilitation therapies.

2 Related Works

Considering that assistive robots work in direct contact with the user, it is necessary to develop communication channels that allow natural interaction between robots and users. Information obtained from the user's physical, affective, sensorial, and cognitive states can be used by the robot to provide efficient assistance [19, 20].

Different interfaces may be used to establish a natural and intuitive HREI. Interface is defined as the hardware and software link that connect two dissimilar systems, e.g. robot and human [21]. Here, sensors play an important role as they obtain the information that supports the interaction between the assistive robot and the user. In addition, actuators can be used to transmit information back to the user to improve the HRI [20].

SWs' interfaces are used to obtain information about the human locomotion [16], the human motion intention [13], the perception of the environments [22] and the navigation [23]. In this context, the interfaces not only are used to obtain information about the user but also of the environment, thus reaching for information at physical, cognitive, and sensorial levels. Leveraging multiple interfaces is fundamental to gather information used by interaction strategies and its controllers to improve the HREI, guaranteeing safe and comfortable interaction between human and SW.

Recent advances in physical HRI have shown the potential and feasibility of robots for active and safe workspace sharing and collaboration with humans [20, 24]. Considering that the user and robot share the same space in an SW, the physical contact between them is essential during navigation. For this reason, the physical Human-Robot interface (pHRi) should be used to generate an easier and natural flow of information, that improve the human-environment communication.

The pHRi information is used within control strategies to produce a collaborative and cooperative work between the user and the SW, which are the components involved in this kind of interface. Here, the environment has a secondary role because the information flow is focused on the user-SW aggregate. Both the user and the SW information feed the controller to execute a specific task, which is shared by them. In SWs, the main role of a pHRi is exchanging information to empower the human locomotion, in addition to having the option of generating a haptic feedback related to the environment information [13, 14, 16]. Therefore, the user's cognitive system is stimulated in a positive way. Usually, the user's gait [25, 26], and the human force is the information involved in this interface because of the direct physical contact [11, 13, 27], or indirect contact through a common object or sensor between the user and the robot [28].

Wachaja et al. [28] proposed an interaction strategy based on a pHRi implemented via a vibration belt worn by the user. It generates a haptic feedback to guide visually impaired individuals across the environment. This kind of vibrotactile interface is also used in the handlebars [28], and in a pair of bracelets located on the user's wrists [29]. Vibration signals indicate the direction to follow, but it is the user who makes the decision on whether to accept the suggestions. This way, the pHRi is used as part of the interaction strategy to transmit the navigation commands. Another kind of pHRi is used in Jimenez et al. [14] to guide visually impaired individuals throughout the environment. In this work, a haptic feedback transmitted during locomotion via the SW's forearm supports indicated the path to be followed while assuring that the user would not deviate from it.

The pHRi is also used on the SWs within the detection processing of the user's motion intentions. For example, taking advantage of the physical contact between the user and the SW, the user's motion intention can be measured using force sensors located under the forearm supporting platforms [13] or in the handlebars of the SW [30, 31]. This kind of sensors are also used to detect a comfortable user position in the SW [16, 32]. Regarding the human gait, the laser range finder (LRF) sensor is used as a safety rule for user [13], and to detect the user's motion intention [33, 34], or to empower the information obtained from the force sensors [16] in order to improve the motion intention detection. It is necessary to take into account that pHRi should not induce an additional higher cognitive process in the user, as this can produce a complex process to recognize the navigation commands.

Usually, cognitive Human-Robot interfaces (cHRi) are directly linked to physical interfaces [21]. An association between the user's skills, versatility, knowledge, and intelligence, combined with the pHRi gives advantages to the collaborative and cooperative work to improve the HREI. The use of cHRi is fundamental in order to get a natural bidirectional communication channel between humans and robots [21]. Therefore, the interplay of cHRi and pHRi should allow the user to be aware of the possibilities of the robot while allowing him to maintain control of the robot at all times [16]. This way, the human-robot cognitive interaction as a consequence of the process between the cHRi and the pHRi, generates an intuitive and natural HREI where the user has a main role.

In SWs, the role of the cHRi is to transmit the robot's cognitive information to the user in order to perform the walker functionalities, that is to say, the user observes the state of the walker through a feedback sent by an object/device used as the interface [16]. All the flow of information needed between the user and the robot in order to perform a task can be linked to the cHRi. In addition, such interface may assist the user to chose the destination [35], to follow recommendations [30] and/or make decisions about the path [13] that should be taking for a safe navigation during walking.

Interaction strategies for SW targeting post-stroke patients have mainly focused on the use of physical interfaces. Morone et al. [18] presented a study performed with patients with mild subacute stroke using the iWalker. The iWalker is an SW with motorized wheels and force sensors positioned in the handlebars as a pHRi. In this study, Morone et al. [18] found that the use of the iWalker increased balance and gait stability. Nevertheless, the interaction strategy used by Morone et al. [18] is not detailed and data analysis is rather focused on patient stability and balance, lacking in the evaluation of the interaction parameters. Loterio et al. [17] presented a follow-in-front interaction strategy – based on a cHRi – for SW in a study focused on post-stroke individuals. The discussion presented by the authors does not address aspects related to the HRI per se, since their focus was on performing a neuromuscular analysis comparing the effects of SW usage and free gait.

Hellström et al. [36] presented a study with a passive SW to guide post-stroke patients in the presence of obstacles in the environment. Separate breaks were mounted in the rear wheels to change the speed of the SW when obstacles are detected, creating a haptic pHRi to indicate to the patient how to avoid the obstacle. Hellström et al. [36] observed that the patients reported positive opinions regarding the SW while also noting that the proposed unimodal interaction strategy considerably reduces walking speed when compared with a regular rollator. Ye et al. [37] presented an interaction strategy for SWs based on a pHRi to be employed in gait rehabilitation for post-stroke patients. Nevertheless, their system was validated only with healthy individuals. A similar approach can be observed in Mun et al. [38]. Multiple interaction strategies for SWs have been validated with populations affected by other diseases, such as ataxia and cerebral palsy [39, 40].

It is important to note that the development of HRI strategies based on pHRi focused on post-stroke patients presents several particularities. Asymmetric gait patterns and asymmetric upper limbs forces are characteristics commonly observed in such a population, which pose challenges in terms of signal processing for extracting movement intent. Thus, the use of more sophisticated interfaces coupled with pHRi is fundamental to provide proper interaction to post-stroke patients. In this work, we present two use cases with post-stroke patients using a SW under two different multimodal HRI strategies capable of offering guidance.

3 Materials and Methods

3.1 The UFES Smart Walker

The robotic platform used in this work is the UFES Smart Walker (shown in Fig. 1), developed at UFES/Brazil. An

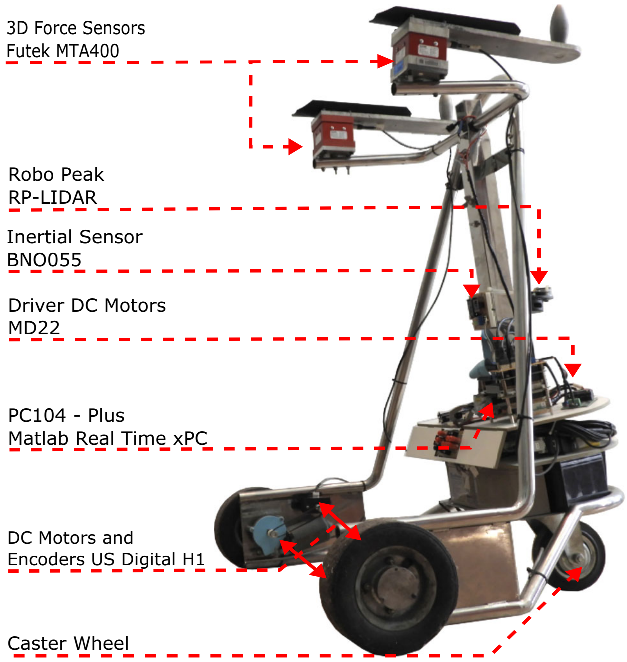

Fig. 1 Smart Walker of UFES/Brazil

embedded computer PC/104-Plus standard (1.67 GHz Atom N450, 2 GB of RAM memory) is used to control and perform processing tasks. This application is integrated into a real-time architecture based on Matlab® Simulink Real-Time xPC Target Toolbox. A laptop is used to program the embedded computer and to store experimental data when necessary. It is connected to the PC/104-Plus by Ethernet exchanging UDP/IP packets.

The UFES Smart Walker possesses the kinematics of a unicycle robot, with a pair of differential rear wheels driven by DC motors and a front caster wheel. The sensory hardware is composed by a pair of H1 (US Digital, USA) encoders and an inertial sensor BNO055 (Adafruit, USA), used to capture the walker's velocities and orientation and feed the odometry algorithm; two triaxial force sensors, MTA400 (Futek, USA), positioned under each forearm supporting platform; and two LRF sensors: a URG-04LX (Hokuyo, Japan), placed on the back of the walker to capture user's legs position, and a RP-Lidar (RoboPeak, China), installed in the front to obtain environmental information.

3.2 Cognitive and Physical Human-robot Interfaces for Multimodal Interaction

The UFES SW possess two main interaction layers, one for human-robot interaction and another one for interaction with the environment. Interaction strategies developed to the UFES SW usually rely on both physical and cognitive interfaces based on two kinds of sensors. A pair of 3D force sensors are used both as pHRi and cHRi to determine the user's motion intentions and provide haptic feedback. A laser range finder (LRF) sensor (Hokuyo URG-04LX) is used to obtain the distance between the user's legs and the walker [16], being a cHRi.

The human-robot-environment interaction is based on environmental and displacement information gathered by a group of sensors. The odometry is determined through a 9 DOF inertial sensor BNO055 and an optical shaft encoders H1 (US Digital, US), which measure the wheels velocities. Both sensors are used to provide the robot's position and orientation in real-time. Another LRF sensor, an RP-LIDAR, is located in front of the SW and is used as a sensory assistant, recovering environmental information to detect obstacles, walls and people.

The interaction layers uses the SW interfaces to establish the communication channels between the user and the walker (see Fig. 2a and b respectively). Figure 2a shows the force sensors located under the forearm supports. Taking advantage of the physical contact between the user and the SW, the control strategies developed generate a haptic feedback to guide the user across the environment. Such a physical interface – or pHRi – detects the motion intention and establishes the human-robot communication. Moreover, this interface

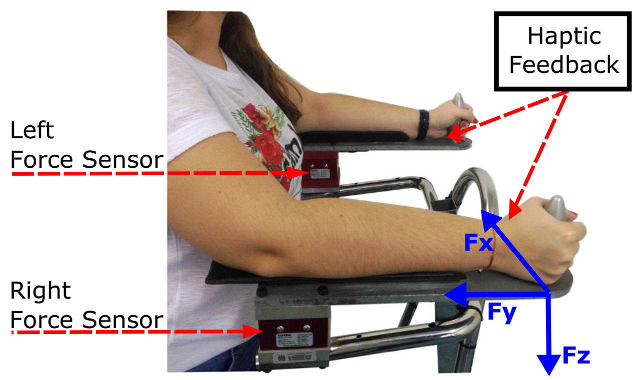

(a)

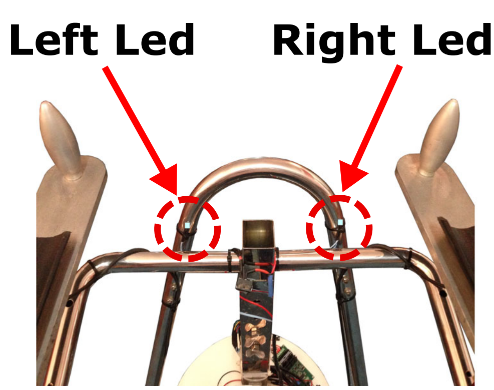

(b)

Fig. 2 SW interfaces. a) Physical and Cognitive interface based on force sensors; b) Visual interface also works as a cognitive interface – or cHRi – as the haptic feedback induces the user to make decisions about the path to follow.

Figure 2b shows the LEDs that are used to complement the information giving by the haptic feedback. The LEDs turn on to recommend a turn direction and is used as a cHRi. In this manner, when the user deviates from a provided path, the corresponding LED turns on to recommend the correct direction. Thus, the SW user is able to decide and command the SW in the right direction.

3.3 Guiding Interaction Strategies

Two multimodal interaction strategies aimed at guiding the user through a path are implemented in the SW. Both use admittance-based controllers to relate user's interaction forces with SW velocities. The first interaction strategy presented in this section is the spatial modulation technique, which was first presented by Jimenez et al. [13]. The second interaction strategy, the virtual torque technique, was first presented by Jimenez et al. [14]. Both strategies take advantage from the physical contact between the user and the SW to generate a haptic feedback and indicate the right path for the user. The main difference is that while the spatial modulation technique aims at indicating the correct path to the user, the virtual torque technique aims at maintaining the user in the path and avoiding any deviations from it.

In the spatial modulation technique, the force sensors (see Fig. 2a) are used to determine the user's motion intention. The signals from the y axis of each sensor are used to define the force and torque applied for the user on the SW, as shown in Eqs. 1 and 2.

$$F(t) = -\frac{F_{L_Y}(t) + F_{R_Y}(t)}{2} \tag{1}$$

$$\tau(t) = -\frac{F_{L_Y}(t) - F_{R_Y}(t)}{2} \times d, \tag{2}$$

where $F_{L_y}(t)$ is the force on the left arm, $F_{R_y}(t)$ is the force on the right arm, and d is the distance between sensors [13]. Then, the user signals of force $F(t)$ and torque $\tau(t)$ can be used in a standard admittance-based controller to obtain the linear $\nu_c(t)$ (see Eq. 3) and angular $\omega_c(t)$ (see Eq. 4) velocities, which are used as the references velocities for the SW. This way, the user can establish a desired linear and angular velocity for locomotion.

$$\nu_c(t) = \frac{F(t) - m_\nu \dot{\nu_c}(t)}{d_\nu}, \tag{3}$$

$$\omega_c(t) = \frac{\tau(t) - m_\omega \dot{\omega_c}(t)}{d_\omega}, \tag{4}$$

where the masses (m_ν and m_ω) and damping (d_ν, d_ω) parameters can modify the HREI dynamics. In other words, in the standard admittance-based controller, while the interaction forces have direct impact on movement, the dynamics of the system are modulated by the masses and dumping parameters. Thus, the use of fixed parameters provides a given interaction characteristic (e.g., the user may feel that the smart walker is lighter/heavier or easier/harder to accelerate), and the user can roam freely around the environment. Here, the two multimodal interaction strategies presented modify the standard admittance-based controller to provide guidance. The spatial modulation technique modulates the masses and damping parameters to make it easier to follow that path and harder when the user deviates from it. The virtual torque technique modifies Eq. 4 by substituting the user-generated torque $\tau(t)$ by a virtual torque $\tau_v(t)$ (see Eq. 12) to ensure that the user will remain on the path.

To guide the user through the desired path, both interaction strategies use the path following controller proposed by Andaluz et al. [41]. Since the robot must respond to the user, we use Andaluz et al. [41] kinematic controller closed loop equation to obtain a desired orientation to the walker, instead of a desired velocity as would be suitable for an autonomous robot. Establishing a desired orientation is a key step that allows us to modulate the admittance-based controller to provide guidance. The closed loop equation from Andaluz et al. [41] can be seen in Eq. 5.

$$\begin{bmatrix} \dot{x}_d \\ \dot{y}_d \end{bmatrix} = \begin{bmatrix} \nu_r cos\theta_p + l_x tanh\left(\frac{k_x}{l_x}\tilde{x}\right) \\ \nu_r sin\theta_p + l_y tanh\left(\frac{k_y}{l_y}\tilde{y}\right) \end{bmatrix}, \tag{5}$$

where ν_r is the path reference velocity; θ_p is the path reference orientation, defined by the tangent of the nearest point to the path; l_x and l_y determine the saturation limits of the position error; k_x and k_y are constant gains that establish the linear zone of the position error; and $\tilde{x}$ and $\tilde{y}$ are the position errors of the SW with respect to the path [13]. The desired orientation θ_d for the SW is calculated from the orthogonal vectors $\dot{x}_d$ and $\dot{y}_d$ (see Eq. 6).

$$\theta_d = atan\left(\frac{\dot{y}_d}{\dot{x}_d}\right). \tag{6}$$

The orientation error $\tilde{\theta}$ between the SW orientation θ and the desired orientation θ_d can be obtained with the Eq. 7.

$$\tilde{\theta} = \theta_d - \theta \tag{7}$$

The orientation error is needed by the interaction strategies to produce the haptic feedback and guide the user across the path in the spatial modulation and virtual torque techniques. Both interaction strategies are described below.

1. Spatial Modulation Technique. This interaction strategy varies the damping parameter of the admittance controller in real time through a spatial modulation technique. This results in a haptic feedback, which is used to indicate to the user the right direction to follow [13]. In this sense, the SW becomes increasingly difficult to handle when the user deviates from the desired path.

From Eq. 3, the mass m_ν maintain a constant value, and the damping parameter d_ν varies according to an inverted Gauss behavior (see Eq. 8).

$$d_\nu(t) = d_{\nu_{max}} - d_{d_{max}} e^{-\left(\frac{\tilde{\theta}}{\delta_{d_\nu}}\right)^2}, \tag{8}$$

where $d_{\nu_{max}}$ is the maximum limit of $d_\nu(t)$; $d_{d_{max}}$ is the maximum decrease of velocity damping; and δ_{d_ν} is the parameter that determines the width of $d_\nu(t)$ function. This way, when $\tilde{\theta}$ is zero, the damping is minimum, allowing the SW to move with the smallest restriction [13].

Thus, such damping behavior establishes a virtual canal with the user, allowing for movements with less effort. When the user deviates from the path, the d_ν value increases and the SW's linear velocity $\nu_c(t)$ decreases. The user perceives this change through the haptic feedback due to the physical contact with the SW. This sense, the SW's maneuverability is difficult and he/she has to put more effort to keep moving with the walker [13].

Regarding $\omega_c(t)$ (see Eq. 4), the restriction for the mass parameter is also used here, thus, m_ω has a constant value. The damping parameter d_ω varies in the time according to the Eq. 9.

$$d_\omega(t) = d_{i_\omega} + G_{d_\omega} tanh\left(\frac{1}{P_{d_\omega}} \tau\tilde{\theta}\right), \tag{9}$$

where d_{i_ω} is the initial damping value in the angular velocity; G_{d_ω} is the gain variation of the torque damping, and P_{d_ω} is the variation slope [13]. However, it is necessary to take into account in Eq. 9 the following restriction to avoid negative values of $d_\omega(t)$:

$$d_{i_\omega} > G_{d_\omega},$$

Here, if the user tries to correct the SW orientation when exist an orientation error $\tilde{\theta}$, the d_ω value decreases, and as a consequence, $\omega_c(t)$ increases. Nonetheless, if the user induces a torque in the wrong direction, the d_ω value increases and the $\omega_c(t)$ decreases, thus, the user needs to do more effort to keep turning in such direction.

To determine d_ω, it is necessary to take into account: (i) $d_i\omega$, as the average of the maximum and minimum desired damping; (ii) $G_d\omega$, as half of the difference of the maximum and minimum desired dumping; (iii) $P_d\omega$, which is empirically defined based on the desired haptic feedback and resulting interaction. We refer the reader to Jimenez et al. [13] for an in-depth discussion on this matter.

This way, the spatial modulation of $d_\nu(t)$ and $d_\omega(t)$ allows for adjusting the controller's parameters to modify the user experience, as the zone for the free mobility can be as narrow – or as large – as needed. Also, the changes in $d_\nu(t)$ and $d_\omega(t)$ values are reflected on the haptic feedback, as the user feels increased difficulty when deviating from the desired path, and based on such sensation, can make decisions about the direction to follow to stay on the path.

2.Virtual Torque Technique. When using this interaction strategy, the user cannot change voluntarily the SW's orientation, as this depends on a virtual torque $\tau_\nu(t)$ generated by the control strategy. This guarantees that the user does not deviate from a provided path. However, the user can establish a comfortable (linear) velocity $\nu_c(t)$for locomotion through the interaction forces, being able to start or stop the movement when necessary.

This virtual torque strategy leverages the user's forces (see Eq. 1) to determine the linear velocity of the SW (as shown in Eq. 3). The mass m_ν and damping d_ν parameters have constant values, which can be adjusted to modify the user experience and the human-robot-environment interaction dynamics.

In this case, the angular velocity of the SW depends on the generated virtual torque, which is calculated from two virtual forces (see Eqs. 10 and 11 respectively). The orientation error (see Eq. 7) is the spatial information used to define such virtual forces, which are after used to establish the virtual torque (see Eq. 12). The equations are shown below:

$$F_1(t) = k(1 + tanh(\tilde{\theta})), \tag{10}$$

$$F_2(t) = k(1 - tanh(\tilde{\theta})), \tag{11}$$

$$\tau_\nu(t) = \frac{F_1(t) - F_2(t)}{2}.d, \tag{12}$$

where k is the gain constant used for setting forces, and d is the distance between the force sensors (see Fig. 2).

The virtual torque $\tau_\nu(t)$ is used to calculate the angular velocity of the SW, as shown in Eq. 13.

$$\omega_c(t) = \frac{\tau_\nu - m_\omega \dot{\omega_c}(t)}{d_\omega}, \tag{13}$$

The value of the mass m_ω and damping d_ω can be adjusted, as they also participate in the HREI dynamics.

Despite allowing the user to establish pace, the human turn intention is not taken into account in this strategy. In this sense, when the user desires to turn and the path does not have a curve, through the haptic feedback, the user perceives that this is a wrong decision and corrects his/her intention. For this reason, not taking into account the human turn intention is not a restriction, as it is a way to explore the haptic feedback to indicate the right path to follow.

The walker has two safety rules. The first one is not permit negative linear velocities to avoid a possible collision between the user and the SW. In the second rule, the linear velocity was limited to 0.25 m/s. Such safety rules were implemented to guarantee the user's safety during navigation with the SW.

4 Case Studies

Two volunteers with post-stroke participated in the study, which were recruited at the Espirito Santo Physical Rehabilitation Center - CREFES, located in the city of Vila Velha, Espírito Santo-Brazil. The Volunteers signed the Free and Informed Consent Form (Number CAAE: 64797816.7.000 0.5542), which was approved by the Ethics Committee of Federal University of Espirito Santo - UFES. Before starting the experiments, the International Physical Activity Questionnaire - Short Form (IPAQ-SF) was applied in order to assess the level of physical activity of each individual to classify them as physically active or sedentary. Both patients were classified as sedentary.

Furthermore, the following criteria will be observed for the inclusion of Volunteers:

- Fits into category 2 or greater than 2 of the Functional Ambulation Category (FAC) scale described by [43], which is used to assess the amount of human care, rather than devices, required for ambulation;
- Ability to stand erect and with elbows at 90^o when using the smart walker;
- Cognitive and language skills sufficient to understand and follow the test instructions.

Added to these, they follow the exclusion criteria:

- Individuals who do not have independent gait;
- Volunteers with cardiorespiratory impairment that prevent walking tests;
- Individuals that are not within the height range (1.54 m - 1.74 m).

4.1 Volunteer No. 1

A 48 year old woman (1.65 m height and 68 kg weight; Body Mass Index = 25 kg/m^2), with a history of arterial hypertension and diabetes, had one ischemic stroke in the left hemisphere of the brain 8 months before the experiments. As sequelae, they presented hemiparesis, with spasticity in the right lower limb and upper limb. Their spasticity in the knee joint was classified as level 2 on the Ashworth Modified Scale [42], which indicates more marked increase in muscle tone through most of the range of motion, but the affected parts are easily moved.

The Functional Ambulation Category (FAC), developed by (HOLDEN et al., 1984), was used to determine how much human assistance the patient requires when walking without use of devices. In order to use this scale, the patient walked a short distance, about 10 steps, and was classified as category 2 or as dependent ambulator for physical assistance (patient requires manual contact of no more than one person during ambulation on level surfaces to prevent falling, consisting of continuous or intermittent light touch to assist balance or coordination).

4.2 Volunteer No. 2

A 45 year old woman (1.64 m height and 73 kg weight; Body Mass Index = 27 kg/m^2) had one hemorrhagic stroke in the left hemisphere of the brain 5.5 years before the experiments, resulting from a fall during a seizure. As sequelae, they presented hemiparesis, with spasticity in the right lower limb and upper limb and memory loss. Their spasticity in the knee joints was classified as level 1 on the Ashworth Modified Scale [42], which indicates slight increase in muscle tone, manifested by a catch and release or minimal resistance at the end of the range of motion when the affected parts is moved in flexion or extension.

They were classified in FAC as category 4 or as independent ambulator in level surfaces only (patient can ambulate independently on level surfaces, but requires supervision or physical assistance to negotiate any of the following: stairs, inclines, or non-level surfaces).

4.3 Experimental Protocol

In this study, the goals were to evaluate the HRI, the SW interfaces, and the control strategies developed and implemented on the SW, which allow guiding people through a pre-established path. Data from all of the SW's sensors was recorded. Initially, the Volunteers walked without any assistive device along a 10-meter straight path on a flat surface with a comfortable speed for three times. This way, the volunteer step was observed. Between the performance of one course and another, sufficient pause time was given for each volunteer in order to avoid fatigue and muscle fatigue.

Prior to the tests, the volunteers were advised on their proper use and had a period of time to adapt to the use of the SW doing travels in straight line. Subsequently, the volun-

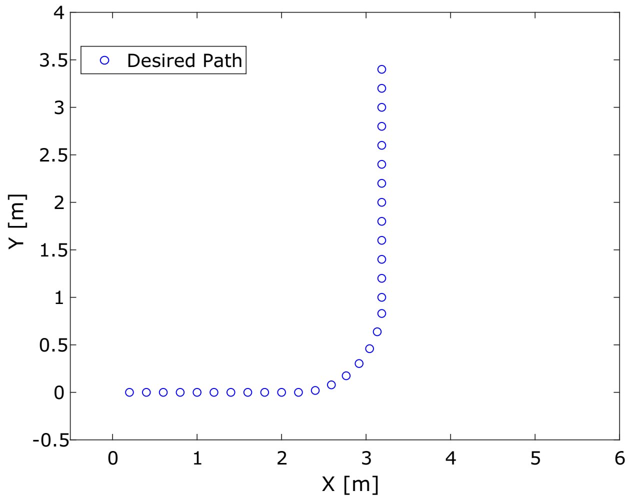

Fig. 3 The pre-established path to be followed by participants

teers used the SW to walked along the pre-established path (see Fig. 3), which was unknown to them. The path is L-shaped and the first straight line is 2.2 m long, followed by a 90^o curve with 1.2 m radius, and a final straight line of 2.5 m long. Moreover, there were no markings on the ground to indicate parts of the path.

The experiment was divided in two parts. In the first one, the SW used the admittance control with spatial modulation, which induces a sensation of hampered maneuverability when steering in a wrong direction. The linear velocity was limited to 0.25 m/s as a security factor. The control parameters values were $m_v = 0.5$, $d_{vmax} = 150$, $d_{dmax} = 140$, $\delta_{dv} = 0.3$, $m_\omega = 0.08$, $d_{i\omega} = 60$, $G_{d\omega} = 59$ and $P_{d\omega} = 1$. All the variables were determined empirically from the experiments.

For the second experiment, the volunteers were instructed to go through the path under the effect of the virtual torque for the angular velocity control. The control parameters values were $m_v = 5$, $d_v = 10$, $m_\omega = 0.5$, $d_\omega = 2$ and $k = 3$. In the same way as the first experiment, all the variables were determined empirically from the experiments.

The Volunteers had to travel across the pre-established path three times using each interaction strategy and understand the interaction between the SW and the user.

4.4 Results and Discussions

The results are presented according to the interaction strategy. First, the results obtained when using the first controller are shown, followed by the second controller.

Spatial modulation technique. In the first part, the volunteers were asked to follow the pre-established path using the SW's physical and cognitive interface under the spatial modulation technique. The two volunteers faced some difficulties in understanding how to operate the SW during the first trial, but that was usually resolved during the second. Figure 4a shows the paths traveled by the Volunteer No. 1 in the three attempts. In the first and third attempt, the volunteer only reached the first straight segment and the turn zone, as the spasticity in their right upper limb hampered the interaction with the SW when turning left. In the second attempt, the volunteer did not manage to follow the path.

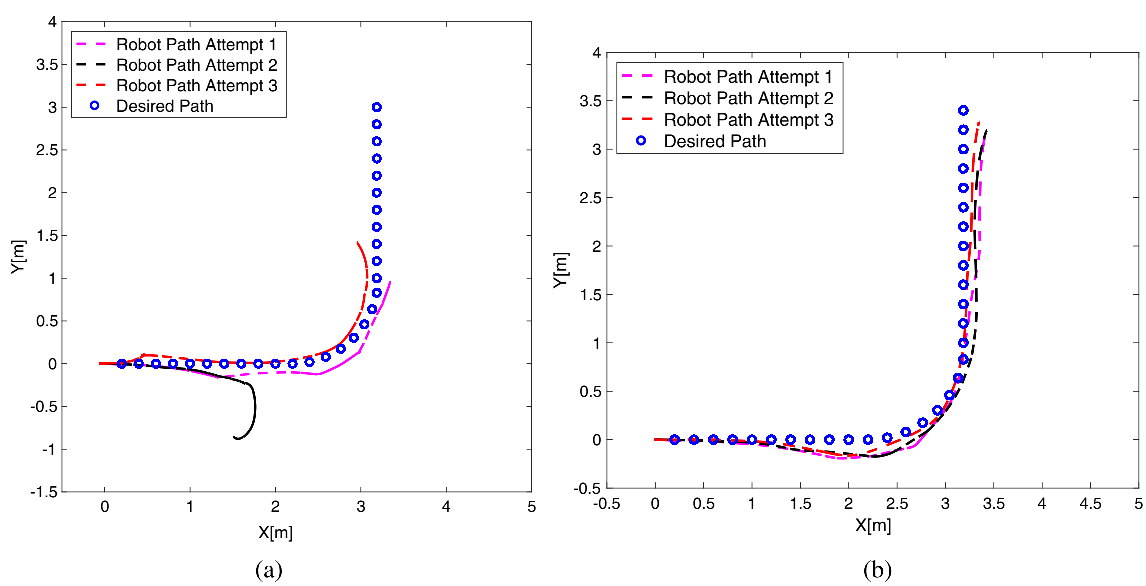

Fig. 4 Following the desired path. Interaction strategy: Spatial modulation technique. a) Volunteer No.1; b) Volunteer No. 2

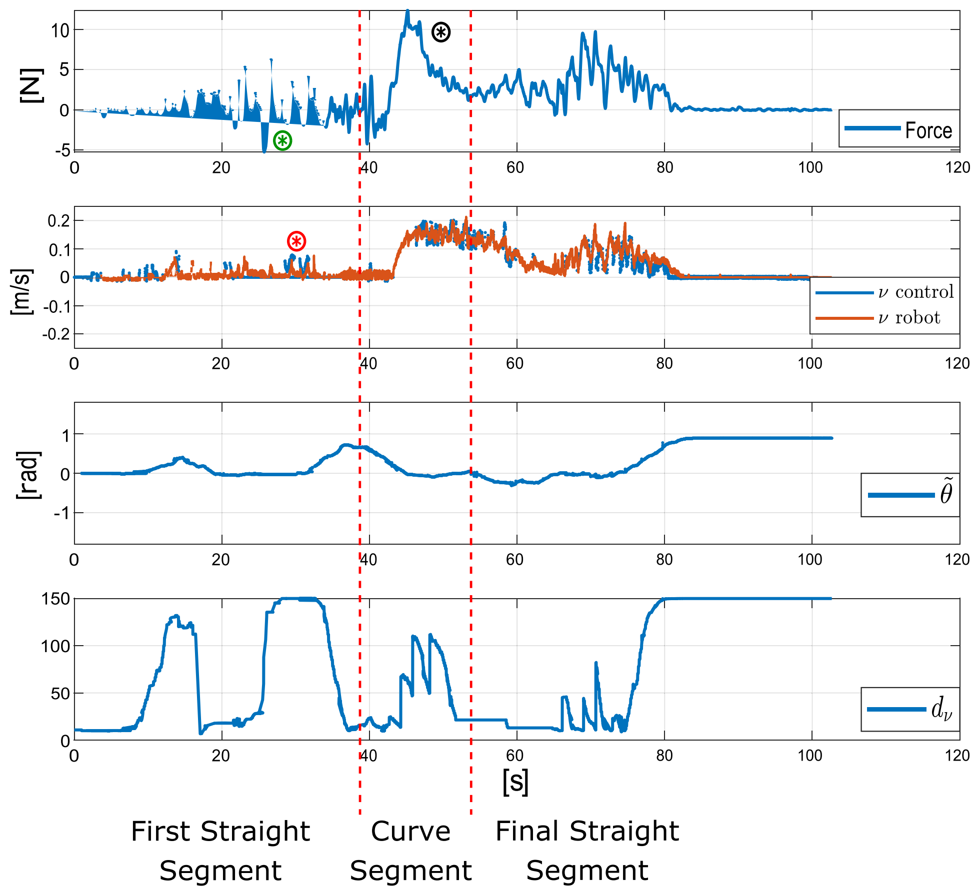

Fig. 5 Volunteer No. 1. Interaction strategy: Spatial modulation technique. Up to down: user's force signal, Control and SW linear velocities, $\tilde{\theta}$ signal, d_ν signal

The Volunteer No. 2 presented better domain over the SW as they reached the end of the path in all of the three attempts, as shown in Fig. 4b. It is necessary taking into account that this Volunteer has more time in therapy than Volunteer No. 1, and as a consequence, they have more control over their body. Volunteer No. 2 understood the interaction way between the user and the SW in this interaction strategy and they could correct the steering when deviating from the path (see the first straight segment, between 0 m to 2.2 m in Fig. 4b).

Figure 5 shows the physical interaction forces between the Volunteer No. 1 and the walker during attempt #3. The Volunteer does not present a continuous locomotion pattern in the first straight segment of the pre-established path, as the force signal is not stable, oscillating between positive and negative values (see red asterisk in Fig. 5). This is reflected in the SW linear velocity, as it changes between 0 m/s and 0.08 m/s. Note here that negative velocity values are not allowed for Volunteer safety (see Fig. 5). Also, in this segment, the Volunteer goes in a wrong direction for a moment (see between 0 *m* and 1 *m* section in Fig. 4a). At that moment, the Volunteer felt the difficulty to go forward with the SW as a consequence of the increment in d_ν signal. They tried to go back to the right direction applying a negative force on the SW (see green asterisk in Fig. 5), but the SW did not respond the motion intention due to the safety rule. During the curve, the Volunteer applied more force on the SW as just could move the left arm voluntarily (see black asterisk in Fig. 5), and due to the increment in d_ν. After such effort, they could not take control over the SW again, and they kept moving in a wrong direction (see the end of the SW travel in Fig. 4a). At this moment, the Volunteer decided to stop their locomotion. For this reason, at the end of Fig. 5, $\tilde{\theta}$ acquired a value different to zero as well as the d_ν signal (see the end of Fig. 5).

The interaction torques during attempt #3 between the Volunteer No. 1 and the SW are shown in Fig. 6. During the first straight segment, the user applied a torque over the SW voluntarily, leading to a deviation from the path (see after black dashed line in Fig. 6). However, they corrected their steering and came back to the desired path. This indicates that the Volunteer understood the interaction form of the strategy implemented. Also, d_ω decreases when they make the decision to turn to the pre-established path (see the red asterisk in Fig. 6). During the curve, the Volunteer tried to follow the path and applied torque in the right direction, but the effort is bigger and not enough to leave the SW over

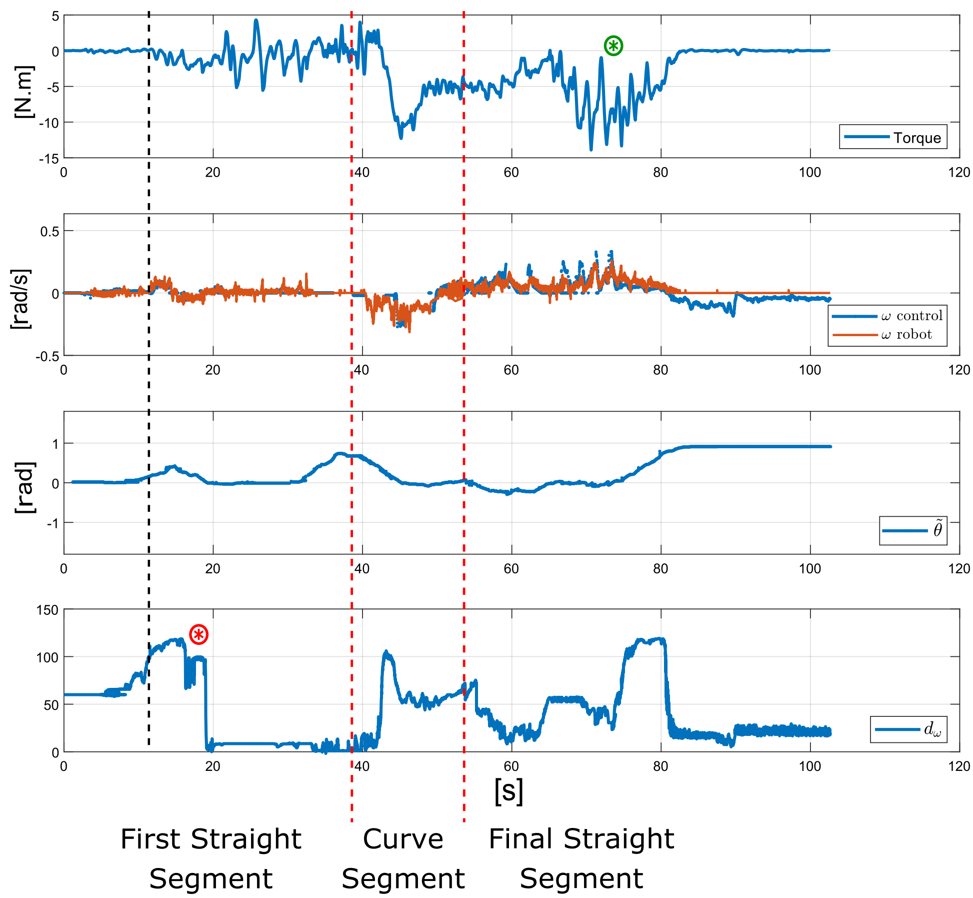

Fig. 6 Volunteer No. 1. Interaction strategy: Spatial modulation technique. Up to down: user's torque signal, Control and SW angular velocities, $\tilde{\theta}$ signal, d_ω signal

the pre-established path. Also, $d\omega$ value decreases when the Volunteer turns in the right direction. However, the Volunteer continued applying torque only over their left arm, and the torque to go back to the path was difficult to do (see the green asterisk in Fig. 6), due to the d_ω value incremented the turn difficulty. Thus, the Volunteer decided no keep moving and the SW end in a wrong orientation.

Regarding Volunteer No. 2, Fig. 7 shows the forces during attempt #3. In this case, the Volunteer goes out of the pre-established path near to the 2 m after beginning the travel (see Fig. 4b). In that moment, through the haptic feedback, the Volunteer feels as the SW decreases its velocity, and the difficulty of maneuvering the SW is increased as the d_v value increased too (see after the black dashed line in the first straight segment, Fig. 7). Once the Volunteer corrects their steering, the difficulty to handle the SW as well as the Volunteer effort decreases, thus, the SW velocity increases. During the turn, the Volunteer has to increase their effort to keep advancing (see the red asterisk in Fig. 7), but, once reached the end of the turn, the needed effort decreases and they could keep moving to the end point of the pre-established path. Despite this Volunteer has spasticity in their upper and lower limbs, the force that they applied on the SW was enough to maneuver the walker in this interaction strategy. Furthermore, they have more time in therapy.

Figure 8 shows the interaction torques between Volunteer No. 2 and the SW for the attempt #3. When the Volunteer deviates from the pre-established path in the first straight segment (see Fig. 4b), they have to apply a torque movement to get the right direction and return to the path. Just after they did the right torque, the d_ω and the Volunteer torque value decreases (see after black dashed line in Fig. 8). Then, the Volunteer had to do a torque to follow the curve, and once they have a good orientation, the SW increase its angular velocity (see the red asterisk in Fig. 8) and the Volunteer can follow over the pre-established path. After turning, the Volunteer continues applying a torque to maintain the SW on the path, but almost at the end of this, the SW has a small orientation error (see Fig. 4b) as a consequence of the torque applied in the curve by the Volunteer.

Despite the Volunteers understood the functionality of this interaction strategy using the haptic feedback, they found it difficult to keep total control over the SW, as this strategy needs the motor control of the two forearms to obtain the user motion intention, and this way, improve the interaction with the SW during navigation.

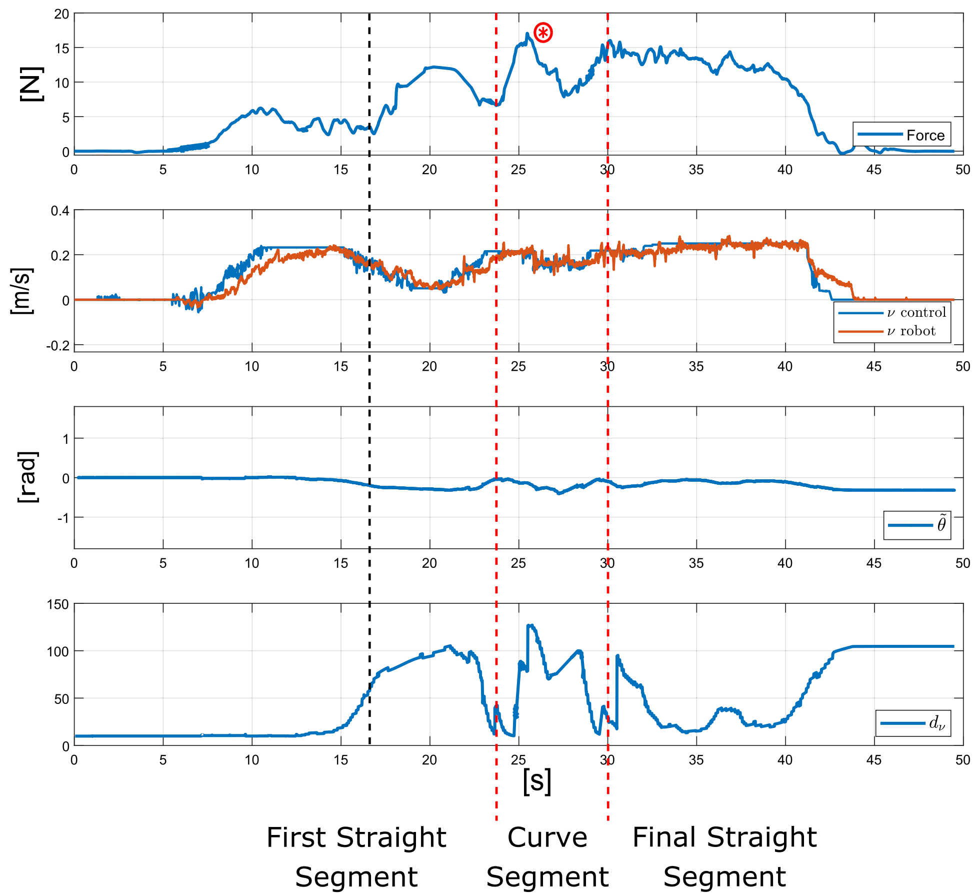

Fig. 7 Volunteer No. 2. Interaction strategy: Spatial modulation technique. Up to down: user's force signal, Control and SW linear velocities, $\tilde{\theta}$ signal, d_ν signal

The visual interface is used to complement the haptic feedback. Figure 9a and b shows the LEDs recommended for each case, which turn on when the the orientation error $\tilde{\theta}$ overpass the 0.436 rad. Thus, it became easier for the Volunteer to identify the right direction to navigate. For instance, for the first Volunteer, the LEDs recommended a turn to the right on different occasions, as they navigate around the right of the pre-established path almost all the time (see Fig. 4a). In the case of the Volunteer No. 2, the visual interface recommended the turn two times (see Fig. 9b). This Volunteer corrected the orientation when necessary (see Fig. 4b) and had a better performance with the SW. Overall, the mean linear velocity observed for Volunteer No. 1 and No. 2 were 0.10 $\pm$0.031 m/s and 0.20 $\pm$0.012 m/s, respectively. These results are compatible, albeit lower, with the ones observed by Jimenez et al. [13] when validating the spatial modulation technique with healthy subjects.

Virtual torque technique. When using the SW configured with the virtual torque technique, the Volunteers established comfortable locomotion speeds, as they just had to put force on the SW to keep moving. Figure 10a and b shows the path traveled by each Volunteer respectively. Under this strategy, both Volunteers reached the end of the path in at least one attempt, which indicates that the interaction between the user and the SW in this interaction strategy may be easier, as users have control over the SW during navigation and move through the pre-established path with a good locomotion velocity.

Figure 11 shows the interaction forces and torques on the Volunteer No. 1 during their third attempt. Here, the resulting torque is generated by the control strategy and not by the Volunteer. In general, the torque exerted by the Volunteers does not change during the turn (see curve segment in Fig. 11). Figure 11 displays torque measurements in a similar way as the force signals. As the Volunteer has spasticity in their right limbs, just the left forearm signals can be used to calculate torque and force. On this interaction strategy, the Volunteer can increase or decrease locomotion velocity using the force amount applied to the SW. For example, in the second 20th, they applied more force on the SW and the SW increase its velocity (see after black dashed line in Fig. 11). This can influence in the cognitive system of the Volunteer in a positive way, as they can decide the forward velocity. On the other hand, the Volunteer applied less force on the SW than when using the previous interaction strategy during navigation (see force signals in Fig. 5). This way, the fatigue

Fig. 8 Volunteer No. 2. Interaction strategy: Spatial modulation technique. Up to down: user's torque signal, Control and SW angular velocities, $\tilde{\theta}$ signal, d_ω signal

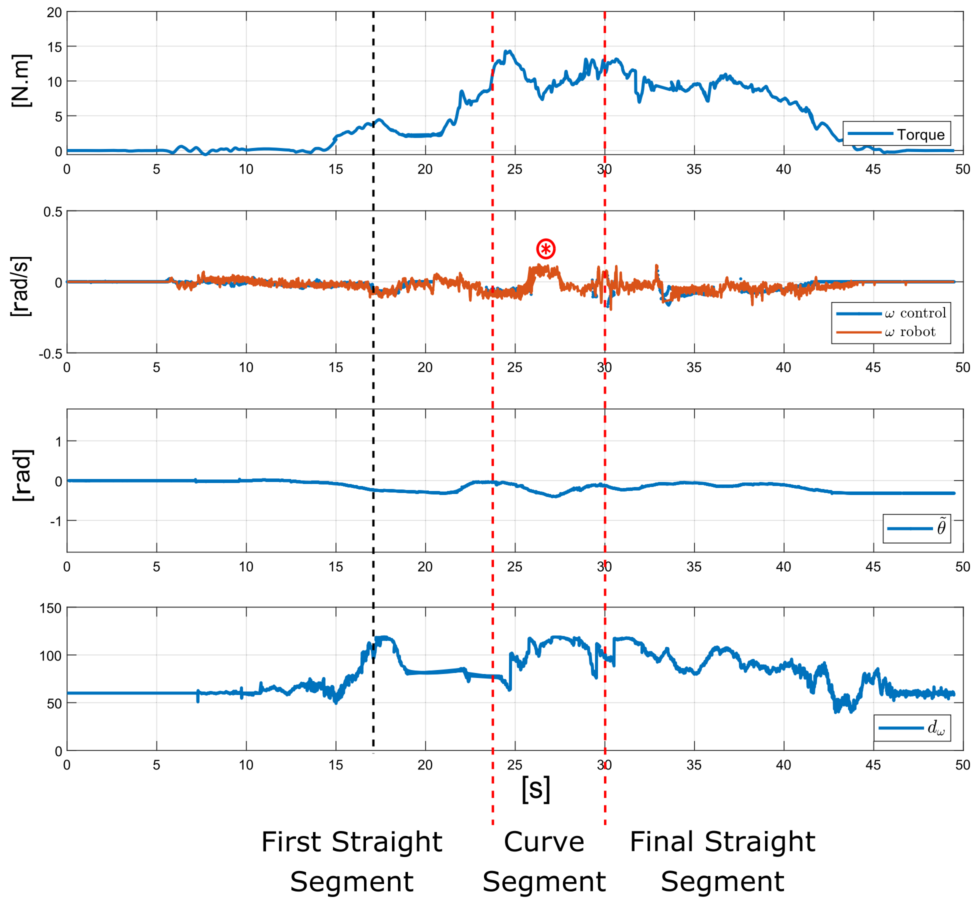

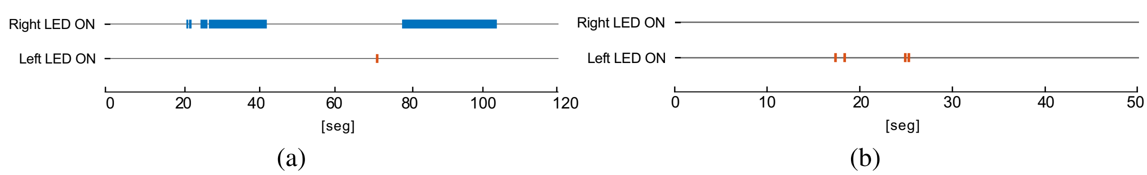

Fig. 9 Recommendations of turn by the visual interface. a) Volunteer No.1, attempt #3; b) Volunteer No. 2, attempt #1

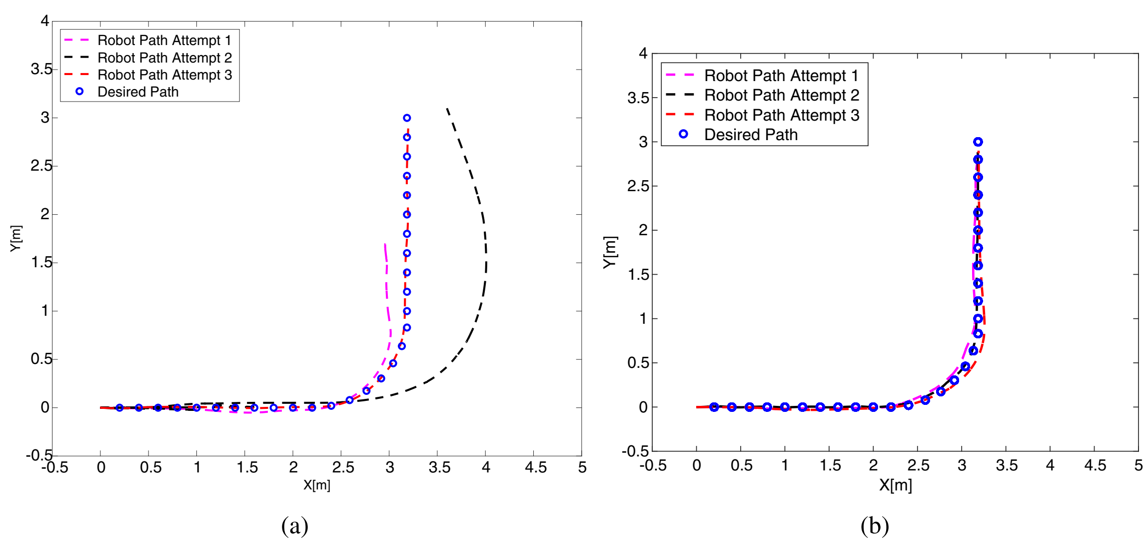

Fig. 10 Following the desired path. Interaction strategy: Virtual torque technique. a) Volunteer No.1; b) Volunteer No. 2

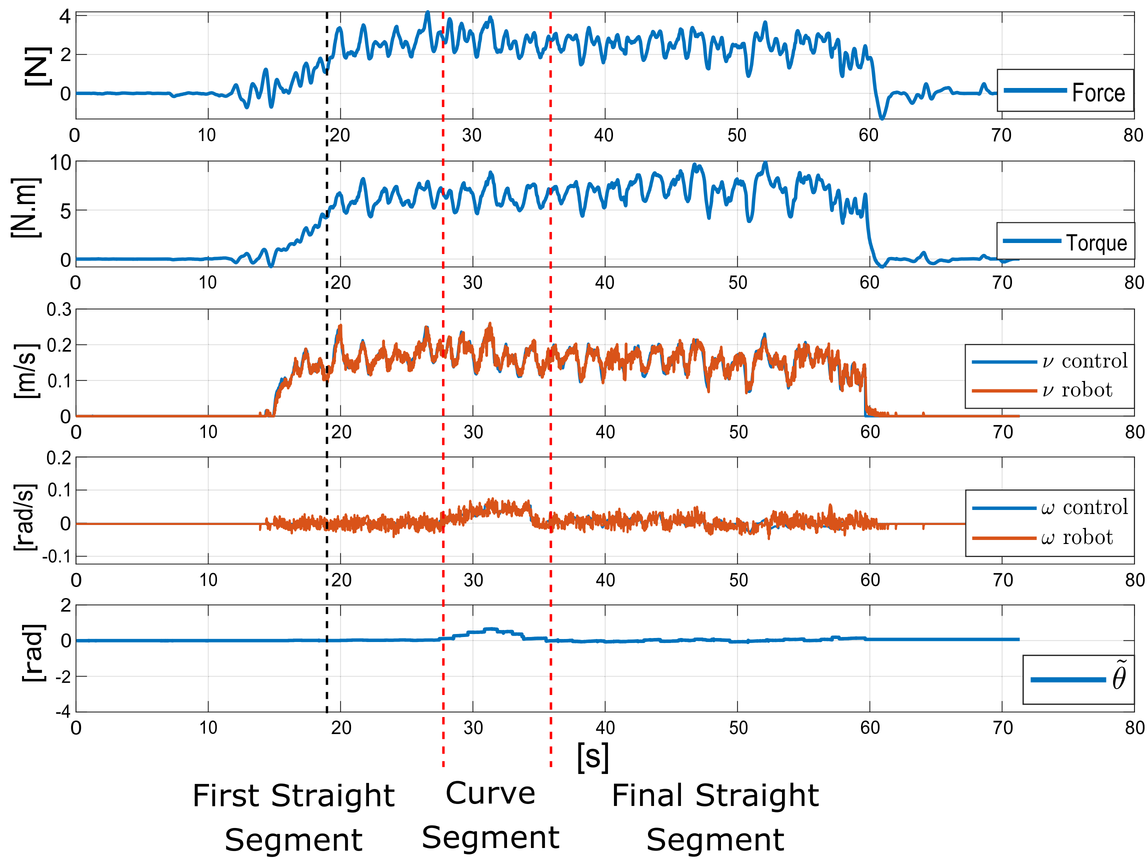

Fig. 11 Volunteer No. 1. Interaction strategy: Virtual torque technique. Up to down: user's force signal, user's torque signal, Control and SW linear velocities, Control and SW angular velocities, $\tilde{\theta}$ signal

observed when using the previous interaction strategy can be avoided. Also, the SW velocity in the second interaction strategy is higher than when was used the spatial modulation technique (see Figs. 5 and 11 respectively).

Figure 12 shows the interaction forces and torques of Volunteer No. 2 when the SW is using the virtual torque technique to guide her in attempt #3. During the first straight segment, the SW increases its velocity when the user increases their force and vice-versa. Just after the curve, the Volunteer applied torque on the SW to change the locomotion direction, but this not induce any change on the SW angular velocity (see red asterisk in Fig. 12), as the torque is generated by the control strategy. Also, it can be observed that the Volunteer has a natural stop with the SW at the end of the path. They begin to reduce the force and as a consequence, the SW decreases its velocity.

Overall, the mean linear velocity observed for Volunteer No. 1 and No. 2 were 0.18 ± 0.026 m/s and 0.22 ± 0.0283 m/s, respectively. These results are compatible with the ones observed by Jimenez et al. [14] when validating the virtual torque technique with healthy subjects.

On the other hand, as well as Volunteer No. 1, Volunteer No. 2 also applied less force on the SW using this technique than when used the first interaction strategy. This, plus the fact that each Volunteer arrived at the end of the path indicates that this strategy could benefit the physical rehabilitation of them. In this sense, the interaction between the Volunteers and the SW is easier using the virtual torque technique, as they just have to put force to establish a good locomotion velocity, but also can start or stop the move with the SW when is necessary.

In both multimodal strategies, Volunteers have to make decisions during navigation, thus, these strategies can be also used to cognitive rehabilitation. However, it is necessary to take into account that the first interaction strategy needs more physical and cognitive effort by the Volunteers.

5 Conclusions and Future Work

This work shows two different multimodal interaction strategies to guide post-stroke patients. Both strategies use pHRi

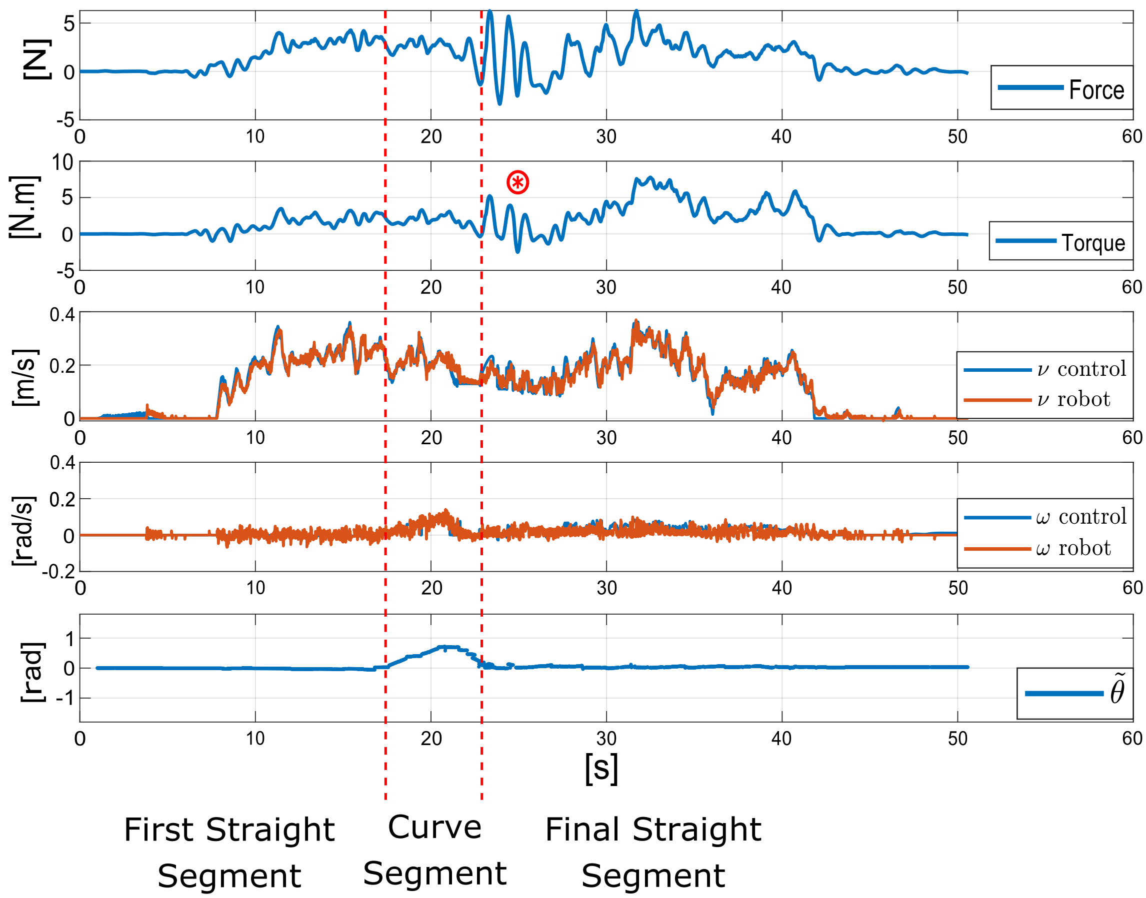

Fig. 12 Volunteer No. 2. Interaction strategy: Virtual torque technique. Up to down: user's force signal, user's torque signal, Control and SW linear velocities, Control and SW angular velocities, $\tilde{\theta}$ signal

and cHRi to communicate the environment information to the SW's user, and thus, improve the HREI.

The haptic feedback allows stimulating the user cognitive system in a positive way, as it is necessary make decisions about the path to follow. In this sense, the SW with the interaction strategies presented here contribute to the physical rehabilitation, but also, to cognitive rehabilitation of people with post-sroke.

The use of the SW during navigation can contribute for avoiding the fatigue that could be presented by stroke patients when using a conventional walker, as in the SW, the user just have to put interaction forces to handle the walker, and not have to do the oscillatory movement that demands the conventional walker to moving. Also, the SW is a robust device that can represent more safety for the patient with post-stroke during navigation, as with the sensors and actuators implemented on the device, many strategies can be developed that improve the HREI.

As future works, new control strategies are being developed to promote the haptic feedback and the use of new interfaces that improve the HREI. In this sense, we are incorporate video cameras on the SW to detect the user's face and utilize its orientation to send commands to the SW, but also, to take the environment information. Thus, keep improving the HREI.

Acknowledgements The authors would like to acknowledge the valuable participation of the volunteers that took part in this study. It is also acknowledged the support given by the School of Engineering, Science and Technology at Universidad del Rosario, Colombia.

Author Contributions All authors (M.F.J., R.C.M., F.L., and A.F.) contributed to the study conception and design. M.F.J. and A.F. conceptualized the study. M.F.J. and R.C.M. designed the methodology. M.F.J. developed the feedback strategies. M.F.J. and R.C.M. conducted the experimental trials and performed data curation and processing. M.F.J. and R.C.M. wrote the original manuscript. M.F.J., R.C.M., and A.F. reviewed and edited the manuscript. A.F. supervised the study. A.F. managed the funding resources. All authors have read and agreed to the published version of the manuscript.

Funding Open Access funding provided by Colombia Consortium. This research is supported by FAPES [grant number 2021-V4J3L, 2022-D48XB and 2022-C5K3H], CNPq [grant number 304049/

2019-0, 403753/2021-0], H2020 European Research Council [grant number 688941] and Universidad del Rosario - Vice Provost of Research and Innovation - Competitive Funds - Medium Grants [grant number IV-FMI001].

Declarations

Ethics approval The ethics committee of the Federal University of Epirito Santo approved the project with the number 2.264.127 to do tests with humans.

Consent to participate Participants were required to fill out an informed consent form to ensure that they have voluntarily expressed their intention to participate in the research, after having understood the naturalness and purpose of the research, the benefits, discomforts, possible risks and alternatives, their rights, and responsibilities. The tests were done in the facilities of the Federal University of Espirito Santo.

Conflict of interest/Competing interests Not applicable. The authors alone are responsible for the content and writing of this article. The authors have no relevant non-financial interests to disclose.

References

1. WHO: World report on ageing and health. Technical report (2015)
2. Van Kammen, K., Boonstra, A.M., Van Der Woude, L.H.V., Reinders-Messelink, H.A., Den Otter, R.: Differences in muscle activity and temporal step parameters between Lokomat guided walking and treadmill walking in post-stroke hemiparetic patients and healthy walkers. J. Neuroeng. Rehabil. (2017). https://doi.org/10.1186/s12984-017-0244-z
3. Shin, S.Y., Kim, Y., Jayaraman, A., Park, H.: Relationship between gait quality measures and modular neuromuscular control parameters in chronic post-stroke individuals. NeuroEngineering Rehabil **18**(58), 1–12 (2021). https://doi.org/10.1186/s12984-021-00860-0
4. Bemelmans, R., Gelderblom, G.J., Jonker, P., de Witte, L.: Socially assistive robots in elderly care: a systematic review into effects and effectiveness. J. Am. Med. Dir. Assoc. **13**(2), 114–120 (2012). https://doi.org/10.1016/j.jamda.2010.10.002
5. Allen, J.L., Kautz, S.A., Neptune, R.R.: Step length asymmetry is representative of compensatory mechanisms used in post-stroke hemiparetic walking. Gait & posture **33**(4), 538–543 (2011). https://doi.org/10.1016/j.gaitpost.2011.01.004
6. Milovanović, I., Popović, D.B.: Principal component analysis of gait kinematics data in acute and chronic stroke patients. Comput. Math. Methods Med. **2012**, 649743 (2012). https://doi.org/10.1155/2012/649743
7. Verma, R., Arya, K.N., Sharma, P., Garg, R.K.: Understanding gait control in post-stroke: implications for management. J. Bodyw. Mov. Ther. **16**(1), 14–21 (2012). https://doi.org/10.1016/j.jbmt.2010.12.005
8. Lennon, O., Tonellato, M., Felice, A.D., Marco, R.D., Fingleton, C., Korik, A., Guanziroli, E., Molteni, F., Guger, C., Otner, R., Coyle, D.: A systematic review establishing the current state-of-the-art, the limitations, and the DESIRED checklist in studies of direct neural interfacing with robotic gait devices in stroke rehabilitation. Frontiers in Neuroscience **14** (2020). https://doi.org/10.3389/fnins.2020.00578
9. Edelstein, J.E.: Assistive devices for ambulation. Phys. Med. Rehabil. Clin. N. Am. **24**(2), 291–303 (2013). https://doi.org/10.1016/j.pmr.2012.11.001
10. Martins, M., Santos, C., Frizera, A., Ceres, R.: A review of the functionalities of smart walkers. Med. Eng. Phys. **37**(10), 917–928 (2015). https://doi.org/10.1016/j.medengphy.2015.07.006
11. Sierra M., S.D., Jiménez, M.F., Frizera-Neto, A., Múnera, M., Cifuentes, C.A.: Control Strategies for Human–Robot–Environment Interaction in Assisted Gait with Smart Walkers, pp. 259–286. Springer, Cham (2022). https://doi.org/10.1007/978-3-030-79630-3_10
12. Sierra M., S.D., Garzón, M., Múnera, M., Cifuentes, C.A.: Human–robot–environment interaction interface for smart walker assisted gait: agora walker. Sensors **19**(13) (2019). https://doi.org/10.3390/s19132897
13. Jiménez, M.F., Monllor, M., Frizera, A., Bastos, T., Roberti, F., Carelli, R.: Admittance controller with spatial modulation for assisted locomotion using a smart walker. Journal of Intelligent and Robotic Systems: Theory and Applications, 1–17 (2018). https://doi.org/10.1007/s10846-018-0854-0
14. Jiménez, M.F., Mello, R.C., Bastos, T., Frizera, A.: Assistive locomotion device with haptic feedback for guiding visually impaired people. Medical Engineering & Physics **80**, 18–25 (2020). https://doi.org/10.1016/j.medengphy.2020.04.002
15. Jiménez, M.F., Scheidegger, W., Mello, R.C., Bastos, T., Frizera, A.: Bringing proxemics to walker-assisted gait: using admittance control with spatial modulation to navigate in confined spaces. Pers. Ubiquit. Comput. (2021). https://doi.org/10.1007/s00779-021-01521-8
16. Cifuentes, C.A., Frizera, A.: Human-robot Interaction Strategies for Walker-assisted Locomotion. vol. 115. Springer, Switzerland (2016). https://doi.org/10.1007/978-3-319-34063-0
17. Loterio, F.A., Valadão, C.T., Cardoso, V.F., Pomer-Escher, A., Bastos, T.F., Frizera-Neto, A.: Adaptation of a smart walker for stroke individuals: a study on semg and accelerometer signals. Research on Biomedical Engineering **33**(4), 293–300 (2017). https://doi.org/10.1590/2446-4740.01717
18. Morone, G., Annicchiarico, R., Iosa, M., Federici, A., Paolucci, S., Cortés, U., Caltagirone, C.: Overground walking training with the i-walker, a robotic servo-assistive device, enhances balance in patients with subacute stroke: a randomized controlled trial. Journal of NeuroEngineering and Rehabilitation **13**(1) (2016). https://doi.org/10.1186/s12984-016-0155-4
19. Amirat, Y., Daney, D., Mohammed, S., Spalanzani, A., Chibani, A., Simonin, O.: Assistance and Service Robotics in a Human Environment. Robot. Auton. Syst. **75**, 1–3 (2016). https://doi.org/10.1016/j.robot.2015.11.002
20. Udupa, S., Kamat, V.R., Menassa, C.C.: Shared autonomy in assistive mobile robots: a review. Disabil. Rehabil. Assist. Technol. **0**(0), 1–22 (2021). https://doi.org/10.1080/17483107.2021.1928778
21. Pons (CSIC), J.L.: Wearable Robots: Biomechatronic Exoskeletons, p. 360. John Wiley & Sons Ltd, Madrid (2008)
22. Palopoli, L., Argyros, A., Birchbauer, J., Colombo, A., Fontanelli, D., Legay, A., Garulli, A., Giannitrapani, A., Macii, D., Moro, F., Nazemzadeh, P., Padeleris, P., Passerone, R., Poier, G., Prat-

tichizzo, D., Rizano, T., Rizzon, L., Scheggi, S., Sedwards, S.: Navigation assistance and guidance of older adults across complex public spaces: the DALi approach. Intel. Serv. Robot. **8**(2), 77–92 (2015). https://doi.org/10.1007/s11370-015-0169-y
23. Aggravi, M., Colombo, A., Fontanelli, D., Giannitrapani, A., Macii, D., Moro, F., Nazemzadeh, P., Palopoli, L., Passerone, R., Prattichizzo, D., Rizano, T., Rizzon, L., Scheggi, S.: A smart walking assistant for safe navigation in complex indoor environments. Biosystems and Biorobotics **11**, 487–497 (2015). https://doi.org/10.1007/978-3-319-18374-9_45
24. Haddadin, S., Croft, E.: Physical human–robot interaction. In: Springer Handbook of Robotics, pp. 1835–1874 (2016). https://doi.org/10.1007/978-3-319-32552-1_69
25. Chongyu, Z., Wenzhi, G., Rongwei, W., Wang, Z., Wu, C.: Deep learning-driven front-following within close proximity: a hands-free control model on a smart walker. In: 2022 International Conference on Robotics and Automation (ICRA), pp. 812–818 (2022). https://doi.org/10.1109/ICRA46639.2022.9811910
26. Scheidegger, W.M., de Mello, R.C., Sierra M., S.D., Jimenez, M.F., Múnera, M.C., Cifuentes, C.A., Frizera-Neto, A.: A novel multimodal cognitive interaction for walker-assisted rehabilitation therapies. In: 2019 IEEE 16th International Conference on Rehabilitation Robotics (ICORR), pp. 905–910 (2019)
27. Mello, R.C., Jimenez, M.F., Ribeiro, M.R.N., Laiola Guimarães, R., Frizera-Neto, A.: On human-in-the-loop cps in healthcare: a cloud-enabled mobility assistance service. Robotica, 1–17 (2019). https://doi.org/10.1017/S0263574719000079
28. Wachaja, A., Agarwal, P., Zink, M., Reyes, M., Möller, K., Burgard, W.: Navigating blind people with walking impairments using a smart walker. Autonomous Robots, 1–19 (2016). https://doi.org/10.1007/s10514-016-9595-8
29. Moro, F., Angeli, A.D., Fontanelli, D., Passerone, R., Prattichizzo, D., Rizzon, L., Scheggi, S., Targher, S., Palopoli, L.: Sensory stimulation for human guidance in robot walkers: a comparison between haptic and acoustic solutions. BT - IEEE International Smart Cities Conference, ISC2 2016, Trento, Italy, 1–6 (2016). https://doi.org/10.1109/ISC2.2016.7580811. Accessed 12-15 Sept 2019
30. Geravand, M., Werner, C., Hauer, K., Peer, A.: An integrated decision making approach for adaptive shared control of mobility assistance robots. Int. J. Soc. Robot. **8**(5), 631–648 (2016). https://doi.org/10.1007/s12369-016-0353-z
31. Morone, G., Annicchiarico, R., Iosa, M., Federici, A., Paolucci, S., Cortés, U., Caltagirone, C.: Overground walking training with the i -Walker, a robotic servo-assistive device, enhances balance in patients with subacute stroke: a randomized controlled trial. J. Neuroeng. Rehabil. **13**, 1–10 (2016). https://doi.org/10.1186/s12984-016-0155-4
32. Chang, Y.-H., Sahoo, N., Chen, J.-Y., Chuang, S.-Y., Lin, H.-W.: Ros-based smart walker with fuzzy posture judgement and power assistance. Sensors **21**(7) (2021). https://doi.org/10.3390/s21072371
33. Valadão, C., Caldeira, E., Bastos-Filho, T., Frizera-Neto, A., Carelli, R.: A new controller for a smart walker based on human-robot formation. Sensors (Switzerland) **16**(7), 1–26 (2016). https://doi.org/10.3390/s16071116
34. Chongyu, Z., Wenzhi, G., Rongwei, W., Wang, Z., Wu, C.: Deep learning-driven front-following within close proximity: a hands-free control model on a smart walker. In: 2022 International Conference on Robotics and Automation (ICRA), pp. 812–818 (2022). https://doi.org/10.1109/ICRA46639.2022.9811910
35. Lacey, G.J., Rodriguez-losada, D.: The evolution of Guido. IEEE Robotics & Automation Magazine **15**(December), 75–83 (2008). https://doi.org/10.1109/MRA.2008.929924
36. Hellström, T., Lindahl, O., Bäcklund, T., Karlsson, M., Hohnloser, P., Bråndal, A., Hu, X., Wester, P.: An intelligent rollator for mobility impaired persons, especially stroke patients. Journal of medical engineering & technology, 1–10 (2016). https://doi.org/10.3109/03091902.2016.1167973
37. Ye, J., Chen, G., Liu, Q., Duan, L., Shang, W., Yao, X., Long, J., Wang, Y., Wu, Z., Wang, C.: An adaptive shared control of a novel robotic walker for gait rehabilitation of stroke patients. In: 2018 IEEE International Conference on Intelligence and Safety for Robotics (ISR), pp. 373–378 (2018). https://doi.org/10.1109/IISR.2018.8535892
38. Mun, K.-R., Lim, S.B., Guo, Z., Yu, H.: Biomechanical effects of body weight support with a novel robotic walker for over-ground gait rehabilitation. Medical & Biological Engineering & Computing **55**(2), 315–326 (2017). https://doi.org/10.1007/s11517-016-1515-8
39. Alazem, H., McCormick, A., Nicholls, S.G., Vilé, E., Adler, R., Tibi, G.: Development of a robotic walker for individuals with cerebral palsy. Disabil. Rehabil. Assist. Technol. **15**(6), 643–651 (2020). https://doi.org/10.1080/17483107.2019.1604827. PMID: 31012754
40. Moreira, R., Alves, J., Matias, A., Santos, C.: Smart and assistive walker – ASBGo: rehabilitation robotics: a smart–walker to assist ataxic patients. In: Robotics in Healthcare, pp. 37–68. Springer, ??? (2019). https://doi.org/10.1007/978-3-030-24230-5_2
41. Andaluz, V.H., Roberti, F., Toibero, J.M., Carelli, R., Wagner, B.: Adaptive dynamic path following control of an unicycle like mobile robot. In: Intelligent Robotics and Applications, pp. 563–574. Springer, ??? (2011). Chap. 56. https://doi.org/10.1007/978-3-642-25486-4_56
42. Chen, C.-L., Chen, C.-Y., Chen, H.-C., Wu, C.-Y., Lin, K.-C., Hsieh, Y.-W., Shen, I.-H.: Responsiveness and minimal clinically important difference of modified ashworth scale in patients with stroke. European journal of physical and rehabilitation medicine **55**(6), 754–760 (2019). https://doi.org/10.23736/s1973-9087.19.05545-x
43. Holden, M.K., Gill, K.M., Magliozzi, M.R. and et al.: Clinical gait assessment in the neurologically impaired, reliability and meaningfulness. Physical Therapy, **64**, 35–40 (1984). https://doi.org/10.1093/ptj/64.1.35

Publisher's Note Springer Nature remains neutral with regard to jurisdictional claims in published maps and institutional affiliations.

Mario F. Jimenez received the B.Sc. degree in Electronics Engineering and the Industrial Control Engineering Master's degree From the Universidad de Ibagué, Colombia, in 2005 and 2012 respectively. In 2018, he received his Ph.D. from the Federal University of Espírito Santo, Vitoria, Brazil. In 2019 he was a researcher in the Signal Analysis Research (SAR) Laboratory at Toronto Metropolitan University. He is currently an Assistant Professor in the School of Engineering, Science, and Technology at Universidad del Rosario, Bogotá, Colombia. His research interests include Human-Robot-Environment interaction, assistive and rehabilitation robotics, and social robotics.

Ricardo C. Mello received the B.Sc., M.Sc., and Ph.D. degrees in electrical engineering from the Federal University of Espírito Santo (UFES), Brazil, in 2015, 2018, and 2020, respectively. He is currently an Assistant Professor with the Electrical Engineering Department, UFES. His Ph.D. thesis dealt with practical aspects of cloud robotics research and his research resulted recently in a book published in Springer's STAR series. His research interests include cloud robotics, networked systems, autonomous systems, and human-robot interaction.

Flavia Loterio graduated in Pharmacy in 2012 and holds a Master's degree (2015) and a Ph.D. (2019) in Biotechnology from the Federal University of Espírito Santo - UFES (Vitoria/Brazil). Her research expertise encompasses areas such as electromyography, gait analysis, and post-stroke hemiparesis gait.

Anselmo Frizera-Neto received the B.S. degree in electrical engineering from the Federal University of Espirito Santo (UFES), Vitória, Brazil, in 2006, and the Ph.D. degree in electronics from the Universidad de Alcalá, Spain, in 2010. From 2006-2010, he was a Researcher with the Bioengineering Group, Spanish National Research Council (CSIC). He is currently a Professor at the Department of Electrical Engineering, UFES. His research interests include rehabilitation robotics, human-machine interaction, and movement analysis.